TECHNISCHE MECHANIK, Band 24, Heft 3-4, (2004), 185– 197
Manuskripteingang: 24. Februar 2004

Harmonic Balance and Averaging Techniques for Stick-Slip Limit-Cycle Determination in Mode-Coupling Friction Self-Excited Systems

This work is dedicated to Professor Friedrich Rimrott for commemorating his outstanding contributions to mechanics, his inspiration, his valuable advice and his heartfelt friendship.

N. Hoffmann, S. Bieser, L. Gaul

A minimal model for mode-coupling friction induced instability with Coulomb-type frictional nonlinearity is set up to investigate the applicability and quality of approximative methods to determine the limit cycles of unstable system configurations. It turns out that - due to the multi-degree-of-freedom nature of the mode-coupling instability - harmonic balance approaches yield reasonable results only if applied carefully, i.e. with respect to the special effects of the nonlinearities under consideration. The Krylov-Bogoliubov-Mitropolsky approach yields good results in a straightforward manner, the technique is however formally much more cumbersome.

1 Introduction

In a large number of mechanical systems self-excited structural vibrations occur as a consequence of structural instabilities and nonlinear system properties. For self-excited friction induced oscillations essentially four different instability mechanisms have been described in literature: First, a friction coefficient decreasing with relative sliding velocity may lead to negative damping and consequently to an oscillatory instability of the steady sliding state. Second, mode-coupling (sometimes also referred to as binary flutter or displacement dependent friction force instability) may destabilize the steady sliding state also for constant friction coefficients. Third, sprag slip, and fourth the follower force nature of the friction force have been identified as fundamental mechanisms for friction self-excited vibrations. All of these mechanisms are amply described in literature (Spurr, 1961; Popp and Stelter, 1990; Ibrahim, 1994; Wallaschek et al., 1999; Gaul and Nitsche, 2001; Gasparetto, 2001; Hoffmann et al., 2002; Hoffmann and Gaul, 2003), a further discussion is therefore not given here. Also when it comes to the systems' nonlinearities, a lot of work has already been conducted, especially on the role of the nonlinearity inherent in friction laws of e.g. the Coulomb type, also in combination with further structural nonlinearities.

Recently the mode-coupling instability has received some attention in the context of technical applications in industry. However, although the instability mechanism of the steady sliding state seems now to be understood rather well (cf. e.g. to Hoffmann et al. (2002); Hoffmann and Gaul (2003)), the evolving dynamics in the nonlinear regime has not yet received much attention. In technical applications the state-of-the-art procedure for modelling and simulating the nonlinear effects of such self-excited vibrations usually consists in setting up large-scale nonlinear finite element (cf. e.g. to Allgaier et al. (2002)) or elastic multi-body models (e.g. Schroth (2003)) and performing time integrations. Even with today's computational capabilities, the corresponding computation times often amount to values that make the application of this direct computational approach in everyday engineering work unfeasible. The objective of the present work therefore is to evaluate alternative approximative techniques to determine basically the amplitudes of the limit cycles that evolve from mode-coupling unstable systems. Of course many approaches have been developed to analyze the dynamic behavior of nonlinear systems (cf. especially to the text of Nayfeh and Mook (1995) for a comprehensive review), in the present context we will apply the simplest techniques available, which are capable to capture the essential nonlinear features: Harmonic Balance and the technique of Krylov-Bogoliubov-Mitropolsky.

The paper is organized as follows: First a simple two-degree-of-freedom model is introduced that may be taken as a minimal model for a mode-coupling unstable system. Second two variants of the technique of Harmonic Balance and the technique of Krylov-Bogoliubov-Mitropolsky are applied to the system to determine the finite-amplitude

limit cycles. The results are then compared and an outlook is given with respect to the applicability of approaches like the ones considered for systems with considerably more degrees of freedom.

2 The Model Problem

For the present conceptual study it is sufficient to formulate a simple two-degree-of-freedom model and investigate its stability behavior and limit-cycle dynamics. A graphical interpretation of the model used for the present work is given in figure 1. The model may be thought of as a single point mass sliding over a conveyor belt, mainly held in position by two linear springs k_1 and k_2 parallel and normal to the belt surface, k_2 may be regarded as the physical contact stiffness between the objects in relative sliding motion. Moreover, there is another linear spring k (oriented at an oblique angle of 45^o relative to the normal direction) leading to off-diagonal entries in the model's stiffness matrix, which has already earlier turned out to be necessary for the appearance of mode-coupling instability, cf. Hoffmann et al. (2002). For the friction a Coulomb model is assumed, where the frictional force F_t is proportional to the normal force F_n exerted at the friction interface, $F_t = \mu F_n$, where μ is the kinetic coefficient of friction taken to be constant.

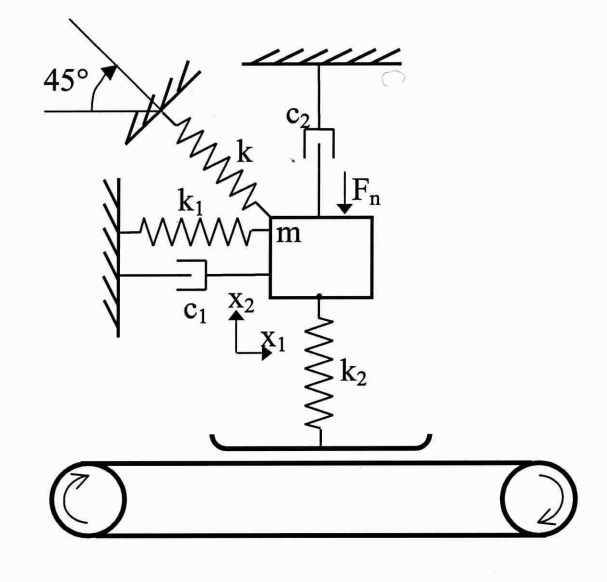

Figure 1. Two-degree-of-freedom model.

Since the normal force at the friction interface is linearly related to the displacement x_2 of the mass normal to the contact surface, the following equations result:

$$\begin{bmatrix} m & 0 \\ 0 & m \end{bmatrix} \begin{pmatrix} \ddot{x}_1 \\ \ddot{x}_2 \end{pmatrix} + \begin{bmatrix} c_1 & 0 \\ 0 & c_2 \end{bmatrix} \begin{pmatrix} \dot{x}_1 \\ \dot{x}_2 \end{pmatrix} + \begin{bmatrix} k_1 + \frac{1}{2}k & -\frac{1}{2}k \\ -\frac{1}{2}k & k_2 + \frac{1}{2}k \end{bmatrix} \begin{pmatrix} x_1 \\ x_2 \end{pmatrix} = \begin{pmatrix} -\mu k_2 x_2 sgn(v_B - \dot{x}_1) \\ F_n \end{pmatrix}, \tag{1}$$

where F_n denotes a constant normal load, v_B stands for the belt speed and linear viscous damping has been assumed. Note that the present model does not capture the possibility of the sliding mass losing contact to the belt (lift-off); it is assumed that the normal load F_n is always large enough to keep the mass in contact with the belt, even when a limit-cycle state is reached.

Before applying approximative techniques to the equations considered it is helpful to take into account the effect that the constant normal load F_n has on the system: F_n causes a static displacement of the mass, which can - by setting all terms involving temporal derivatives to zero - easily determined as

$$x_1^0 = \frac{F_n(\mu k_2 - k/2)}{(k_1 + k/2)(k_2 + k/2) + (\mu k_2 - k/2)k/2},$$

$$x_2^0 = -\frac{F_n(k_1 + k/2)}{(k_1 + k/2)(k_2 + k/2) + (\mu k_2 - k/2)k/2}, \tag{2}$$

where $v_B > 0$ has been assumed. For the subsequent analysis now the deviation from this static equilibrium position is introduced as

$$x_1' = x_1 - x_1^0, \quad x_2' = x_2 - x_2^0. \tag{3}$$

By inserting these relations into eq. (1) and subtracting eq. (2) the equations for x_1' and x_2' result (assuming $v_B > 0$), after some algebra, in a straightforward manner:

$$\begin{bmatrix} m & 0 \\ 0 & m \end{bmatrix} \begin{pmatrix} \ddot{x}_1' \\ \ddot{x}_2' \end{pmatrix} + \begin{bmatrix} c_1 & 0 \\ 0 & c_2 \end{bmatrix} \begin{pmatrix} \dot{x}_1' \\ \dot{x}_2' \end{pmatrix} + \begin{bmatrix} k_1 + \frac{1}{2}k & -\frac{1}{2}k + \mu k_2 \\ -\frac{1}{2}k & k_2 + \frac{1}{2}k \end{bmatrix} \begin{pmatrix} x_1' \\ x_2' \end{pmatrix}$$
$$= \begin{pmatrix} -\mu k_2 (x_2^0 + x_2') \left[sgn(v_B - \dot{x}_1') - 1 \right] \\ 0 \end{pmatrix}, \tag{4}$$

Note that the non-linear right-hand-side term is non-zero only in the case of friction force reversal and then compensates the forces leading to the static solution corresponding to the system's homogeneous part. Since in the following always the deviations from the static equilibrium position will be considered, the primes are from now on again omitted from the variables.

To bring the equations into a more generic form it is convenient to divide by m and to use the relative (Lehr's) damping coefficients $D_i = c_i/(2\omega_i m)$ with $\omega_i^2 = (k_i + k/2)/m$, $i = 1, 2$:

$$\begin{pmatrix} \ddot{x}_1 \\ \ddot{x}_2 \end{pmatrix} + \begin{bmatrix} 2D_1\omega_1 & 0 \\ 0 & 2D_2\omega_2 \end{bmatrix} \begin{pmatrix} \dot{x}_1 \\ \dot{x}_2 \end{pmatrix} + \begin{bmatrix} \omega_1^2 & -\frac{k}{2m} + \mu(\omega_2^2 - k/2m) \\ -\frac{k}{2m} & \omega_2^2 \end{bmatrix} \begin{pmatrix} x_1 \\ x_2 \end{pmatrix}$$
$$= \begin{pmatrix} -\mu(\omega_2^2 - k/2m)(x_2^0 + x_2) \left[sgn(v_B - \dot{x}_1) - 1 \right] \\ 0 \end{pmatrix}. \tag{5}$$

In the context of the present work the focus lies on a fundamental conceptual analysis rather than on parameter studies. Therefore the analysis is, from now on, restricted to the parameters

$$\omega_1^2 = 22.5\ \mathrm{s}^{-2}, \omega_2^2 = 23.0\ \mathrm{s}^{-2}, k/2m = 5\ \mathrm{s}^{-2}, F_n = 9.81\ \mathrm{N}, D_1 = 1.05 \times 10^{-2}, D_2 = 1.04 \times 10^{-2},$$

unless otherwise stated. These values have been chosen to be close to parameters that can be identified from realistic technical applications.

Performing a simple eigenvalue analysis of the homogeneous part of eq. (5) for small vibration amplitudes (i.e. of the left-hand-side of eq. (5)) yields the stability characteristic of the system, as shown in figure 2, where complex eigenvalues are denoted by $\lambda = \sigma + i\omega$.

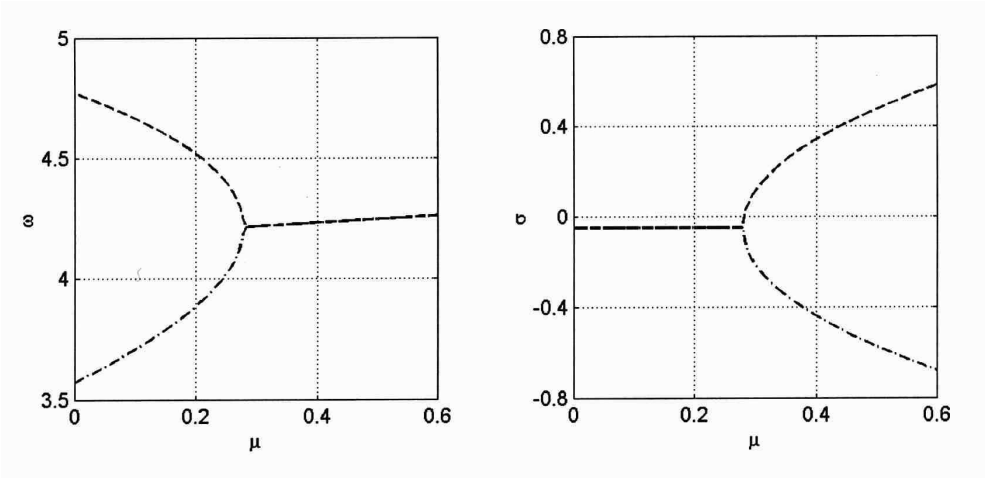

Figure 2. Spectral characteristics of the model system. Imaginary (ω) and real (σ) parts of the resulting eigenvalues $\lambda = \sigma + i\omega$ corresponding to oscillation frequency and growth rate.

For friction coefficients $\mu < 0.28$ the system is characterized by two stable eigenmodes. At $\mu = 0.28$ a merging of modes takes place and for only slightly larger friction coefficients an unstable mode results. This behavior is typical for proportionally damped mode-coupling instability (cf. eg. Hoffmann and Gaul (2003)), a further interpretation is therefore not given here. In the following we will consider the stick-slip limit cycles arising in the

unstable regime, i.e. for $\mu > 0.28$. Figure 3 shows the results of direct time-integration of eq. (5) for $\mu = 0.30$ with initial conditions close to the static equilibrium position. Note that in the beginning the typical exponential oscillatory growth characterizing an oscillatorily linearly unstable system can be seen. This growth persists until the x_1-component of the vibration reaches the velocity of the belt (set here to $v_B = 0.5m/s$) which rapidly limits the amplitude of the oscillation in the x_1-direction, i.e. in the tangential direction at approx. $t \approx 32s$ (left graph of fig. 3). Note however that the x_2-vibration does still increase markedly before saturation at approx. $t \approx 100s$ (middle graph of figure 3). This two-step saturation process is also clearly visible in the phase-plane plot of $\dot{x}_1$ vs. x_1 (right graph of figure 3).

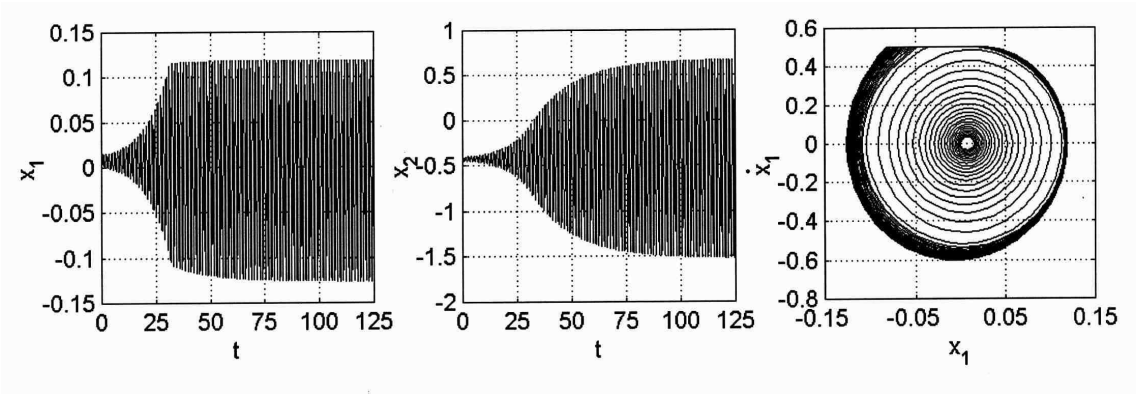

Figure 3. Exemplary results of time integration for the full non-linear system at $< \mu = 0.3$. Transient growth due to instability of the steady sliding state and amplitude saturation for x_1 (left) and x_2 (middle). The right graph depicts a phase-plane plot of $\dot{x}_1$ vs. x_1.

Of course this dynamical behavior can easily be explained: as long as sticking phases do not yet occur, the dynamical behavior is determined by the exponential growth corresponding to the linear instability of the steady sliding state. When the mass first sticks to the belt, the motion tangential to the belt surface (in x_1-direction) is strongly inhibited, in a sense the two-degree-of-freedom system is instantaneously transferred into a single-degree-of-freedom system for the out-of-plane motion (x_2-direction) which is only indirectly affected by the appearance of sticking effects in the x_1-direction: after sticking takes place in the x_1-direction, the x_2-vibration may be considered as a forced vibration with the forcing term stemming from the structurally coupled x_1-vibration. With this picture in mind it may be understood that the times for amplitude saturation of the x_1- and the x_2-component differ substantially. Consequently the amplitude ratio for the saturated x_1- and x_2-oscillations differs from what would have been expected from the unstable system eigenmode. When approximative methods to determine limit-cycle amplitudes are to be considered, it will be crucial that they can cope with this effect and can predict correct amplitudes and amplitude ratios for both tangential x_1- and normal x_2-components.

3 Harmonic Balance Techniques

The technique of Harmonic Balance is one of the classical approaches to determine limit-cycle amplitudes in nonlinear vibration problems. Since the general approach is well known, cf. e.g. to Nayfeh and Mook (1995), we will in the following focus on the specific aspects of the technique in the present context of mode-coupling. It turns out that - as could be expected - the most simple adaptation of Harmonic Balance (presented in the following sub-section) leads to some substantial shortcomings in the results, which can be overcome by a slightly modified approach presented subsequently.

3.1 Application of Conventional Harmonic Balance

To approximately solve equations (5) the following ansatz is chosen:

$$\begin{aligned} x_1 &= x_1^d + A x_1^s \sin(\omega t), \\ x_2 &= x_2^d + A[x_2^s \sin(\omega t) + x_2^c \cos(\omega t)], \end{aligned} \tag{6}$$

where x_1^d and x_2^d denote constant static displacement changes resulting from the oscillation, A denotes the dimensionless limit-cycle amplitude to be determined and x_1^s, x_2^s and x_2^c denote the sine and cosine components of

the system's unstable complex eigenvector after scaling it for computational convenience such that $x_1^c = 0$. The assumption underlying this ansatz is of course that the non-linear limit-cycle oscillation will basically resemble the oscillation corresponding to the exponential growth in the linearly unstable parameter regime and the effect of the non-linearity will mainly lead to this oscillation saturating at a certain amplitude level, represented by an amplitude factor A. With this the right-hand-side non-linear terms of equation (5) read

$$\begin{aligned} & -\mu(\omega_2^2 - k/2m)[sgn(v_B - \dot{x}_1) - 1](x_2^0 + x_2) \qquad (7) \\ & = -\mu(\omega_2^2 - k/2m)[sgn(v_B - A\omega x_1^s \cos(\omega t)) - 1][x_2^d + x_2^0] \\ & -\mu(\omega_2^2 - k/2m)A[sgn(v_B - A\omega x_1^s \cos(\omega t)) - 1][x_2^s \sin(\omega t) + x_2^c \cos(\omega t)], \end{aligned}$$

where static and time-dependent terms have been separated. From these terms only the constant and first harmonic components, determined by integration over one oscillation period $T = 2\pi/\omega$ in the style of Fourier analysis, will be taken into account in the Harmonic Balance approach, cf. e.g. to Magnus and Popp (1997). This leads, after some lengthy but basically straightforward algebra, to the contributions:

$$\begin{aligned} a_1 &= \frac{1}{T}\int_0^T \left(-\mu(\omega_2^2 - k/2m)\right)[sgn(v_B - A\omega x_1^s \cos(\omega t)) - 1](x_2^d + x_2^0)\, dt \qquad (8) \\ &= \frac{2\omega\mu(\omega_2^2 - k/2m)}{\pi}(x_2^d + x_2^0)t_c, \\ a_2 &= \frac{1}{T}\int_0^T \left(-\mu(\omega_2^2 - k/2m)A\right)[sgn(v_B - A\omega x_1^s \cos(\omega t)) - 1](x_2^s \sin(\omega t) + x_2^c \cos(\omega t))\, dt \qquad (9) \\ &= \frac{2\mu(\omega_2^2 - k/2m)A}{\pi}x_2^c \sin(\omega t_c), \\ N_1^s &= \frac{2}{T}\int_0^T \sin(\omega t)\left(-\mu(\omega_2^2 - k/2m)\right)[sgn(v_B - A\omega x_1^s \cos(\omega t)) - 1](x_2^d + x_2^0)\, dt = 0, \qquad (10) \\ N_1^c &= \frac{2}{T}\int_0^T \cos(\omega t)\left(-\mu(\omega_2^2 - k/2m)\right)[sgn(v_B - A\omega x_1^s \cos(\omega t)) - 1](x_2^d + x_2^0)\, dt \qquad (11) \\ &= \frac{4\mu(\omega_2^2 - k/2m)}{\pi}(x_2^d + x_2^0)\sin(\omega t_c), \\ N_2^s &= \frac{2}{T}\int_0^T \sin(\omega t)\left(-\mu(\omega_2^2 - k/2m)A\right)[sgn(v_B - A\omega x_1^s \cos(\omega t)) - 1](x_2^s \sin(\omega t) + x_2^c \cos(\omega t))\, dt \qquad (12) \\ &= \frac{\mu(\omega_2^2 - k/2m)Ax_2^s}{\pi}(2\omega t_c - \sin(2\omega t_c)), \\ N_2^c &= \frac{2}{T}\int_0^T \cos(\omega t)\left(-\mu(\omega_2^2 - k/2m)A\right)[sgn(v_B - A\omega x_1^s \cos(\omega t)) - 1](x_2^s \sin(\omega t) + x_2^c \cos(\omega t))\, dt \qquad (13) \\ &= \frac{\mu(\omega_2^2 - k/2m)Ax_2^c}{\pi}(2\omega t_c + \sin(2\omega t_c)), \end{aligned}$$

where

$$t_c = \begin{cases} \frac{1}{\omega}\arccos\left(\frac{v_B}{Ax_1^s\omega}\right) & for \quad Ax_1^s\omega > v_B \\ 0 & \quad\;\; Ax_1^s\omega \le v_B \end{cases} \qquad (14)$$

has been used to abbreviate the anyway lengthy expressions. Using the terms so obtained, an approximation of the system's non-linear parts, i.e. the right-hand-side of equations (5), up to the first harmonic contributions, can be written down as

$$a + N_2^s \sin(\omega t) + N\cos(\omega t),$$

where again $a = a_1 + a_2$ and $N = N_1^c + N_2^c$ have been used for abbreviation purposes. Using this harmonic expression and changing into an obvious matrix notation, the equations of motion in reduced form may be formulated as

$$\mathbf{M}\ddot{\mathbf{y}} + \mathbf{C}\dot{\mathbf{y}} + \mathbf{K}\mathbf{y} = \begin{pmatrix} a_0 + N_2 \sin(\omega t) + N \cos(\omega t) \\ 0 \end{pmatrix} \equiv \mathbf{R}, \tag{15}$$

where $\mathbf{y} = (x_1, x_2)^T$, $\mathbf{R}$ denotes the right-hand-side vector and the mass, damping and stiffness matrices M, C and K are set up according to equation (5).

Now the right-hand-side term $\mathbf{R}$, representing the forcing due to the non-linear system properties, is expressed in terms of equivalent damping and stiffness forces as

$$\mathbf{R} = \widetilde{\mathbf{C}}\dot{\mathbf{y}} + \widetilde{\mathbf{K}}\mathbf{y}, \tag{16}$$

such that equations (15) can be rewritten as

$$\mathbf{M}\ddot{\mathbf{y}} + \widehat{\mathbf{C}}\dot{\mathbf{y}} + \widehat{\mathbf{K}}\mathbf{y} = 0, \tag{17}$$

where $\widehat{\mathbf{C}} = \mathbf{C} - \widetilde{\mathbf{C}}$ and $\widehat{\mathbf{K}} = \mathbf{K} - \widetilde{\mathbf{K}}$. Inserting the ansatz of equation (6) into equations (16), comparing coefficients for the sine, cosine and constant terms and denoting the matrix coefficients of $\widetilde{C}$ and $\widetilde{K}$ as C_{ij} and K_{ij} leads to the following set of equations to determine $\widetilde{C}$ and $\widetilde{K}$:

$$\begin{aligned} -C_{12}A\omega x_2^c + K_{11}Ax_1^s + K_{12}Ax_2^s &= N_2^s\,, \\ K_{22}Ax_2^s - C_{22}A\omega x_2^c + K_{21}Ax_1^s &= 0\,, \\ C_{12}A\omega x_2^s + C_{11}A\omega x_1^s + K_{12}Ax_2^c &= N\,, \\ C_{21}A\omega x_1^s + K_{22}Ax_2^c + C_{22}A\omega x_2^s &= 0\,, \\ K_{11}x_1^d + K_{12}x_2^d &= a_0\,, \\ K_{21}x_1^d + K_{22}x_2^d &= 0\,. \end{aligned} \tag{18}$$

Obviously the system is underdetermined. There are only six equations to determine ten unknowns. This problem does not appear for single-degree-of-freedom problems, where the method of harmonic balance is usually applied. In order to solve the equations the system will therefore be restricted without loss of generality, since later only the energy functional of the resulting system of equations is evaluated and the restriction may be regarded as an equivalence transformation not influencing the final results. Setting the off-diagonal elements of $\widetilde{C}$ and $\widetilde{K}$ to zero the following solution can be obtained:

$$\begin{gathered} K_{11} = N_2^s/Ax_1^s,\;\; K_{22} = K_{12} = K_{21} = 0, \\ C_{11} = N/A\omega x_1^s,\;\; C_{22} = C_{12} = C_{21} = 0, \\ x_1^d = a_0 Ax_1^s/N_2^s,\;\; x_2^d = 0. \end{gathered} \tag{19}$$

With these coefficients now the energy functional of equation (17) is set up by multiplication with $\dot{\mathbf{y}}^{\mathbf{T}}$ from the left:

$$\frac{d}{dt}\left[\frac{1}{2}\dot{\mathbf{y}}^\top\mathbf{M}\dot{\mathbf{y}} + \frac{1}{2}\mathbf{y}^\top\widehat{\mathbf{K}}^{\mathbf{s}}\mathbf{y}\right] + \dot{\mathbf{y}}^\top\widehat{\mathbf{K}}^{\mathbf{n}}\mathbf{y} + \dot{\mathbf{y}}^\top\widehat{\mathbf{C}}\dot{\mathbf{y}} = 0. \tag{20}$$

Note that here $\widehat{\mathbf{K}}$ has been decomposed into its symmetric ($\widehat{\mathbf{K}}^{\mathbf{s}}$) and anti-symmetric ($\widehat{\mathbf{K}}^{\mathbf{n}}$) part. To determine the constant limit-cycle amplitude A, constant energy solutions of equation (20) have to be obtained, which leads to the condition that the forcing terms vanish when averaged over one vibration amplitude. After some algebra this condition results in

$$\int_0^{\frac{2\pi}{\omega}} \left(\mu(\omega_2^2 - k/2m)\dot{x}_1 x_2 + (2D_1\omega_1 - C_{11})\dot{x}_1^2 + (2D_2\omega_2 - C_{22})\dot{x}_2^2\right) dt = 0. \tag{21}$$

Inserting the ansatz functions and solving the integral yields

$$A^2\omega\pi\left(\frac{\mu(\omega_2^2 - k/2m)}{\omega}x_1^s x_2^c + (2D_1\omega_1 - C_{11})x_2^{s\,2} + (2D_2\omega_2 - C_{22})(x_2^{s\,2} + x_2^{c\,2})\right) = 0, \tag{22}$$

which basically represents the work done on the system by the friction and the damping forces over one vibration cycle. In the top left graph of figure 4 this work is plotted for different values of the friction coefficient as a function

of A. For small enough values of A the dissipated work obviously increases with increasing A. For $A > 10$ the behavior changes and for a certain amplitude A_0 the dissipated energy vanishes. This is the limit-cycle amplitude to be determined, since in the saturated steady limit-cycle dissipative and self-exciting forcing have to equal each other when averaged over one vibration cycle.

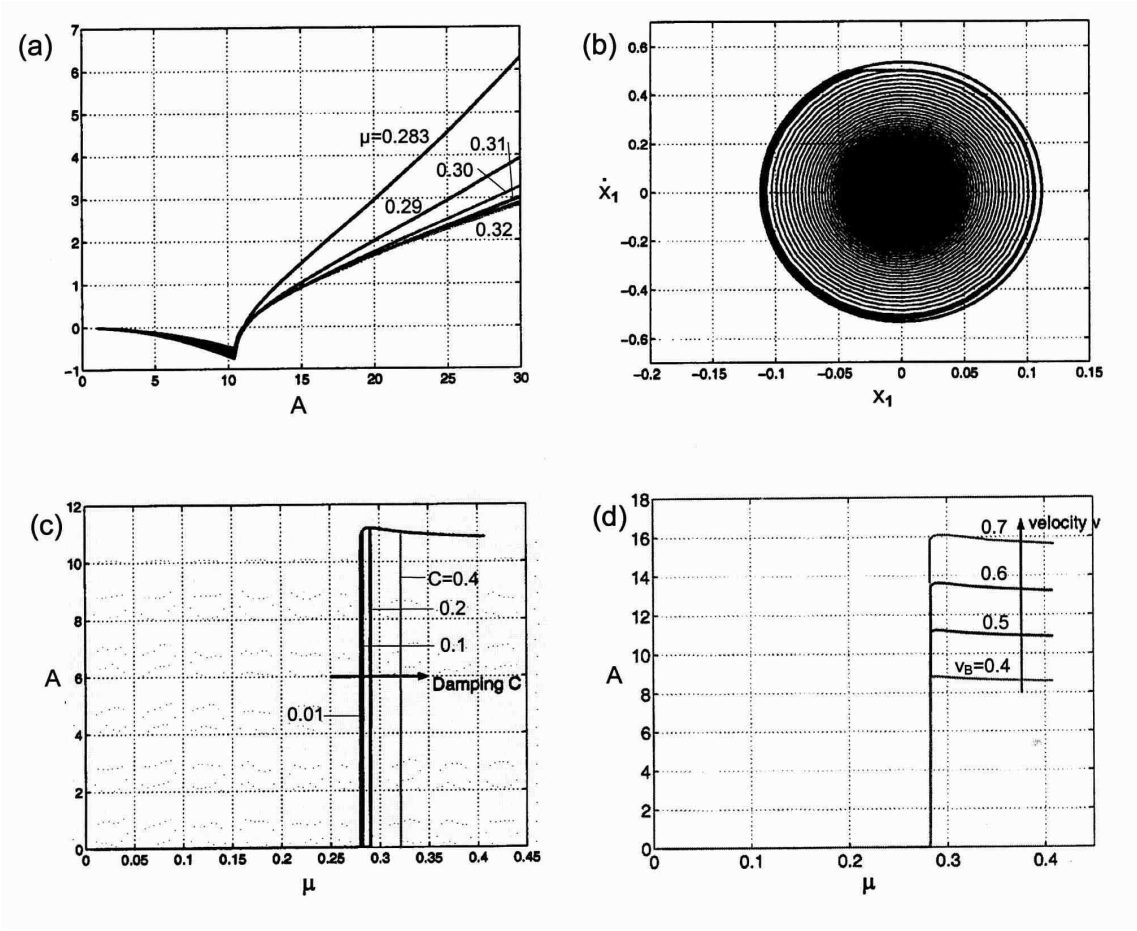

Figure 4. Results of the simple Harmonic Balance approach. (a) Work done vs. vibration amplitude A for supercritical friction coefficients μ. (b) Phase Diagram comparison of direct time-integration (thin lines) and Harmonic Balance (thick circle). (c) Limit-cycle amplitude A vs. friction coefficient for various damping coefficients $C = C_1 = C_2$. (d) Limit-cycle amplitude A vs. friction coefficients μ for various belt velocities v_B.

The bottom left graph of figure 4 shows the effect of damping on the limit-cycle amplitudes A_0. It turns out that increased damping leads to a stabilization of the system, as could have been expected. To complete the picture, the bottom right graph of figure 4 shows the effect of changing belt-velocity v_B on A_0: it turns out that the amplitude increases with belt-velocity, agreeing well with the intuitive picture of the underlying stick-slip behavior. This becomes even clearer, when the phase plane plot of the approximate solution's x_1 component is compared with the result from direct time-integration (top right graph of figure 4). It can be seen that the Harmonic Balance approach described captures the stick-slip limit-cycle behavior of the x_1-direction very well, basically the limit-cycle amplitude is determined largely by the condition that sticking periods appear. This on the other hand also shows the limitations of the approach: it has already been shown in the introductory section by investigating direct time-integration results of the system under consideration that the amplitude ratio of the x_1- and the x_2-components in the saturated limit-cycle state may be markedly different from what can be obtained from the eigenvector analysis. The conventional Harmonic Balance approach presented does however not take this into account. The approximate prediction of the x_2-vibration may therefore be expected to be rather poor, as will be seen below in section 5 where the results of all three techniques presented in this work are compared quantitatively.

3.2 Application of Extended Harmonic Balance

It will become clear below, when the results of the different techniques under consideration are compared, that in the present context the conventional Harmonic Balance approach suffers from its underlying basic one-dimensional nature, whereas the mode-coupling phenomenon is essentially a two-degree-of freedom problem. To account for this two-dimensionality in an approach, that will be called Extended Harmonic Balance from now on, the following modified ansatz is used:

$$\begin{aligned} x_1 &= x_1^d + A_1 x_1^s \sin(\omega t)\,, \\ x_2 &= x_2^d + [A_2^s x_2^s \sin(\omega t) + A_2^c x_2^c \cos(\omega t)], \end{aligned} \tag{21}$$

where instead of a single amplitude factor the oscillatory components are multiplied with the possibly distinct amplitude factors A_1, A_2^s and A_2^c, which allows to take into account changes in the phase and amplitude relations due to the action of nonlinearity. Note that strictly speaking the inclusion of the eigenvector components x_1^s, x_2^s and x_2^c in this ansatz is not really necessary, since each of them is multiplied with an amplitude factor anyway, but in order to keep the analogy to the conventional Harmonic Balance approach they are kept. Note also that in the present approach the frequency ω will not be taken out of the eigenvalue analysis, but will be obtained as a result of the approach.

Basically the procedure now is analogous to conventional Harmonic Balance. The non-linear term, i.e. the friction term on the right-hand-side of equation (5) is projected on its harmonic components resulting in the coefficients - using the same definitions as in the preceding sub-sections:

$$\begin{aligned} N_1^c &= \frac{4\mu(\omega_2^2 - k/2m)}{\pi}(x_2^d + x_2^0)\sin(\omega t_c) \\ N_2^s &= \frac{\mu(\omega_2^2 - k/2m)A_2^s x_2^s}{\pi}\,(2\omega t_c - \sin(2\omega t_c)) \\ N_2^c &= \frac{\mu(\omega_2^2 - k/2m)A_2^c x_2^c}{\pi}\,(2\omega t_c + \sin(2\omega t_c)) \\ a_1 &= \frac{2\omega\mu(\omega_2^2 - k/2m)}{\pi}(x_2^0 - x_2^d)t_c \\ a_2 &= \frac{2\mu(\omega_2^2 - k/2m)A_2^c x_2^c}{\pi}\sin(\omega t_c), \end{aligned} \tag{22}$$

such that approximate equations can again be written down in the form of equations (15). Now the approach differs slightly from conventional harmonic balance. Instead of expressing the non-linearity in terms of damping and stiffness matrices, the ansatz functions are directly inserted into the resulting averaged system equations and a comparison of coefficients is performed for the constant, sine and cosine terms, which yields a nonlinear set of equations:

$$\begin{aligned} -A_1 x_1^s \omega^2 + \omega_1^2 A_1 x_1^s - \frac{k}{2m} A_2^s x_2^s &= N_2^s \\ -A_2^s x_2^s \omega^2 - 2D_2\omega_2 A_2^c x_2^c \omega - \frac{k}{2m} A_1 x_1^s + \omega_2^2 A_2^s x_2^s &= 0 \\ 2D_1\omega_1 A_1 x_1^s \omega - \frac{k}{2m} A_2^c x_2^c &= N_1^c + N_2^c \\ -A_2^c x_2^c \omega^2 + 2D_2\omega_2 A_2^s x_2^s \omega + \omega_2^2 A_2^c x_2^c &= 0 \\ \omega_1^2 x_1^d - \frac{k}{2m} x_2^d &= a_1 + a_2 \\ -\frac{k}{2m} x_1^d + \omega_2^2 x_2^d &= 0 \end{aligned} \tag{23}$$

Here there now are six (non-linear) equations for the six unknowns A_1, A_2^s, A_2^c, ω, x_1^d and x_2^d. The equations can readily be solved by Newton-iterations, the results will be presented below in section 5.

4 Application of the Technique of Krylov and Bogoliubov

The approach of Krylov and Bogoliubov, sometimes also called method of slowly varying amplitude and phase, is well known and well described in literature, cf. eg. to Nayfeh and Mook (1995) or Magnus and Popp (1997). The

following presentation will therefore be kept rather short.

First equations (5) are written in the form

$$\begin{aligned} \ddot{x}_1 + \omega_1^2 x_1 &= g_1, \\ \ddot{x}_2 + \omega_2^2 x_2 &= g_2, \end{aligned} \tag{24}$$

with

$$\begin{aligned} g_1 &= -2D_1\omega_1\dot{x}_1 + (\frac{k}{2m} - \mu(\omega_2^2 - k/2m))x_2 - \mu(\omega_2^2 - k/2m)[sgn(v_B - \dot{x}_1) - 1](x_2^0 + x_2), \\ g_2 &= -2D_2\omega_2\dot{x}_2 + \frac{k}{2m}x_1. \end{aligned}$$

Now the first equation in (24) is expanded with $(\omega^2 - \omega_1^2)x_1$ and the second equation with $(\omega^2 - \omega_2^2)x_2$ in order to obtain the same frequency ω on the left-hand-side of both equations and to redefine the right-hand-side:

$$\begin{aligned} \ddot{x}_1 + \omega^2 x_1 &= (\omega^2 - \omega_1^2)x_1 + g_1 = \tilde{g}_1, \\ \ddot{x}_2 + \omega^2 x_2 &= (\omega^2 - \omega_2^2)x_2 + g_2 = \tilde{g}_2, \end{aligned} \tag{25}$$

The solutions to these equations are now written in the form

$$\begin{aligned} x_1(t) &= A_1(t)\sin(\omega t + \phi_1(t)), \\ x_2(t) &= A_2(t)\sin(\omega t + \phi_2(t)), \end{aligned} \tag{26}$$

and the usual coordinate transformation from the original variables x_1 and x_2 to the new amplitude and phase variables A_1, A_2, ϕ_1 and ϕ_2 is conducted such that the amplitude and phase equations read

$$\dot{A}_1 = \frac{\tilde{g}_1}{\omega}\cos(\theta_1), \quad \dot{\phi}_1 = -\frac{\tilde{g}_1}{A_1\omega}\sin(\theta_1), \tag{27}$$

$$\dot{A}_2 = \frac{\tilde{g}_2}{\omega}\cos(\theta_2), \quad \dot{\phi}_2 = -\frac{\tilde{g}_2}{A_2\omega}\sin(\theta_2),$$

where $\theta_1 = \omega t + \phi_1$, $\theta_2 = \omega t + \phi_2$. Note that the amplitude and phase equations (27) are formally still fully equivalent to equations (25), no approximation has been assumed yet. The approximation process attributed to Krylov and Bogoliubov and sometimes termed the first approximation will be described now: basically it relies on the assumption that the resulting vibrations will be harmonic oscillations with slowly varying amplitude and phase coefficients. This directly leads to the assumption that there are two timescales involved in the resulting dynamics: the fast timescale of the oscillation corresponding to ω and the slow timescale on which amplitudes and phases change. As a consequence of the separation of scales involved in this assumption it seems appropriate to average the amplitude and phase equations (27) over one period of the fast oscillation cycle to obtain averaged amplitude and phase equations:

$$\dot{\bar{A}}_1 = \frac{\omega}{2\pi}\int_0^{\frac{2\pi}{\omega}} \frac{\tilde{g}_1}{\omega}\cos(\theta_1)dt = \frac{1}{2\pi}\int_0^{\frac{2\pi}{\omega}} g_1\cos(\theta_1)dt, \tag{28}$$

$$\dot{\bar{\phi}}_1 = \frac{\omega}{2\pi}\int_0^{\frac{2\pi}{\omega}} -\frac{\tilde{g}_1}{A_1\omega}\sin(\theta_1)dt = -\frac{\omega^2 - \omega_1^2}{2\pi}\frac{\pi}{\omega} - \frac{1}{2\pi A_1}\int_0^{\frac{2\pi}{\omega}} g_1\sin(\theta_1)dt, \tag{29}$$

$$\dot{\bar{A}}_2 = \frac{\omega}{2\pi}\int_0^{\frac{2\pi}{\omega}} \frac{\tilde{g}_2}{\omega}\cos(\theta_2)dt = \frac{1}{2\pi}\int_0^{\frac{2\pi}{\omega}} g_2\cos(\theta_2)dt, \tag{30}$$

$$\dot{\bar{\phi}}_2 = \frac{\omega}{2\pi}\int_0^{\frac{2\pi}{\omega}} -\frac{\tilde{g}_2}{A_2\omega}\sin(\theta_2)dt = -\frac{\omega^2 - \omega_2^2}{2\pi}\frac{\pi}{\omega} - \frac{1}{2\pi A_2}\int_0^{\frac{2\pi}{\omega}} g_2\sin(\theta_2)dt. \tag{31}$$

The remaining integrals have to be evaluated, which is a straightforward, although lengthy procedure, so here only the resulting equations are given:

$$\dot{\bar{A}}_1 = \frac{1}{2\pi}\Big[-2D_1\omega_1\bar{A}_1\pi + \frac{k\bar{A}_2\pi}{2m\omega}\sin(\psi) - \frac{\mu(\omega_2^2 - k/2m)\bar{A}_2}{\omega}\sin(\psi)\big(\pi - 2B - \sin(2B)\big) + \frac{4\mu(\omega_2^2 - k/2m)x_2^0}{\omega}\sin(B)\Big], \tag{32}$$

$$\dot{\bar{\phi}}_1 = -\frac{\omega^2 - \omega_1^2}{2\omega} - \frac{1}{2\pi\bar{A}_1}\cos(\psi)\left[\frac{k\bar{A}_2}{2m}\frac{\pi}{\omega} - \frac{\mu(\omega_2^2 - k/2m)\bar{A}_2}{\omega}\big(\pi - 2B + \sin(2B)\big)\right], \tag{33}$$

$$\dot{\bar{A}}_2 = -\frac{2D_2\omega_2\bar{A}_2}{2} - \frac{k\bar{A}_1}{4m\omega}\sin(\psi), \tag{34}$$

$$\dot{\bar{\phi}}_2 = -\frac{\omega^2 - \omega_2^2}{2\omega} - \frac{k\bar{A}_1}{4\omega m\bar{A}_2}\cos(\psi), \tag{35}$$

where $\psi = \phi_2 - \phi_1$ and $B = arccos(v_B/A_1\omega)$ are used. To determine the amplitudes of the stationary limit-cycle, $\dot{\bar{A}}_1$, $\dot{\bar{A}}_2$ and $\dot{\bar{\phi}}_2 - \dot{\bar{\phi}}_2$ are required to equal zero, which yields

$$0 = 2D_1\omega_1\bar{A}_1\pi + \sin(\psi)\Big(\frac{k\bar{A}_2\pi}{2m\omega} - \frac{\mu(\omega_2^2 - k/2m)\bar{A}_2}{\omega}\big(\pi - 2B - \sin(2B)\big)\Big) + \frac{4\mu(\omega_2^2 - k/2m)x_2^0}{\omega}\sin(B), \tag{36}$$

$$0 = \bar{A}_2 + \frac{k\bar{A}_1}{4\omega D_2\omega_2}\sin(\psi), \tag{37}$$

$$0 = \frac{\omega_2^2 - \omega_1^2}{2\omega} + \cos(\psi)\left[\frac{k\bar{A}_2}{4m\omega\bar{A}_1} - \frac{k\bar{A}_1}{4m\omega\bar{A}_2} - \frac{\mu(\omega_2^2 - k/2m)\bar{A}_2}{2\pi\omega\bar{A}_1}\big(\pi - 2B - \sin(2B)\big)\right]. \tag{38}$$

These three equations can now be used to determine the three unknown A_1, A_2 and ψ.

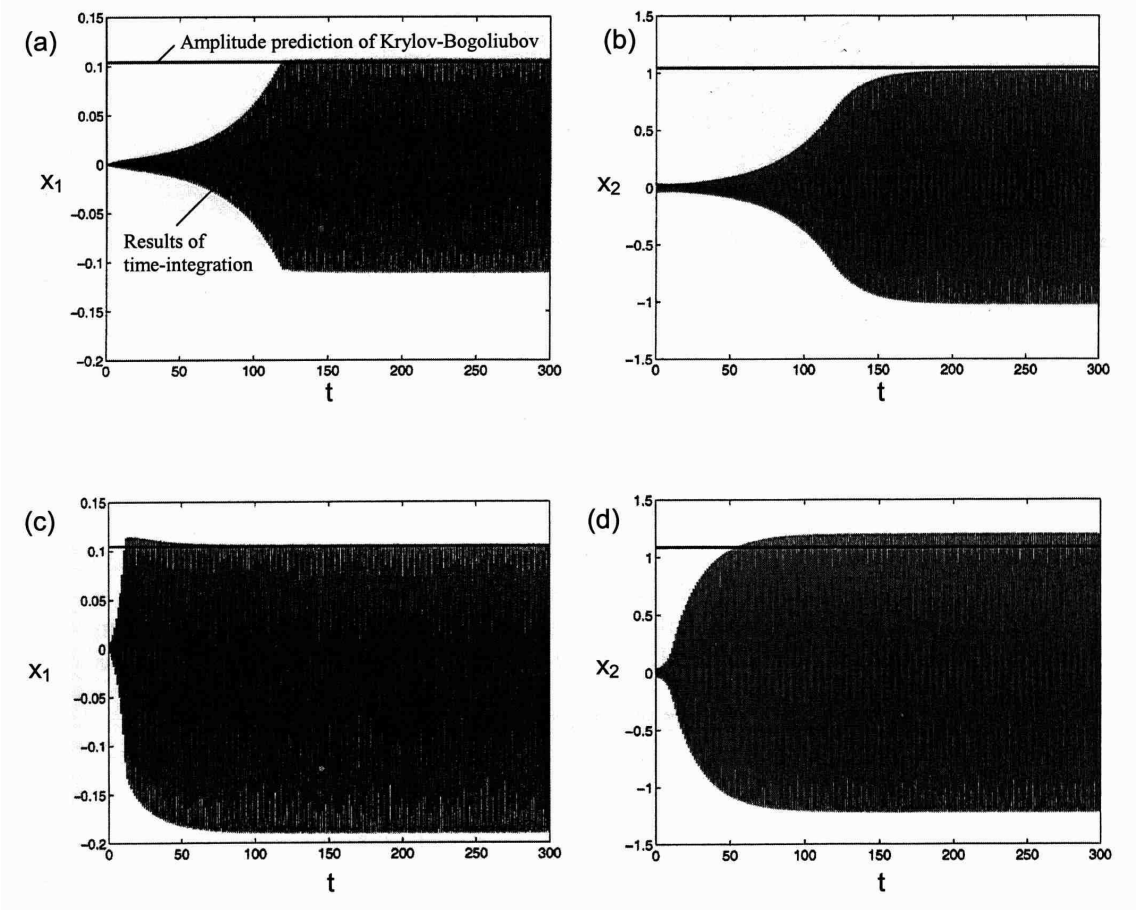

Figure 5. Exemplary results of the Krylov-Bogoliubov approximation: results of direct time integration and predicted oscillation amplitude due to Krylov-Bogoliubov for x_1 and x_2 for $\mu = 0.285$ (a) and (b) and $\mu = 0.35$ (c) and (d).

The non-linear system of equations is solved using Newton iterations. Figure 5 shows typical results: it is obvious that the present approach gives excellent results for friction coefficients μ only marginally above critical (compare figure 5 (a) and (b)), whereas there do remain some discrepancies for larger μ (figure 5 (c) and (d)). These discrepancies can also be understood intuitively rather easily: also the Krylov-Bogoliubov technique assumes basically harmonic behavior for the nonlinear oscillation; for larger μ however the actual stick-slip behavior diverges substantially from harmonic characteristic, explaining the errors to be observed.

5 Comparison of Results

Now it is time to compare the approximation quality of the three approaches presented. To that purpose two parameter studies have been performed. First the damping-factors D_2 in the out-of-plane direction have been varied, second the friction coefficient has been varied. Figure 6 shows the results. For each test case time-integrations have been performed to obtain benchmark values and the approximate techniques have been applied.

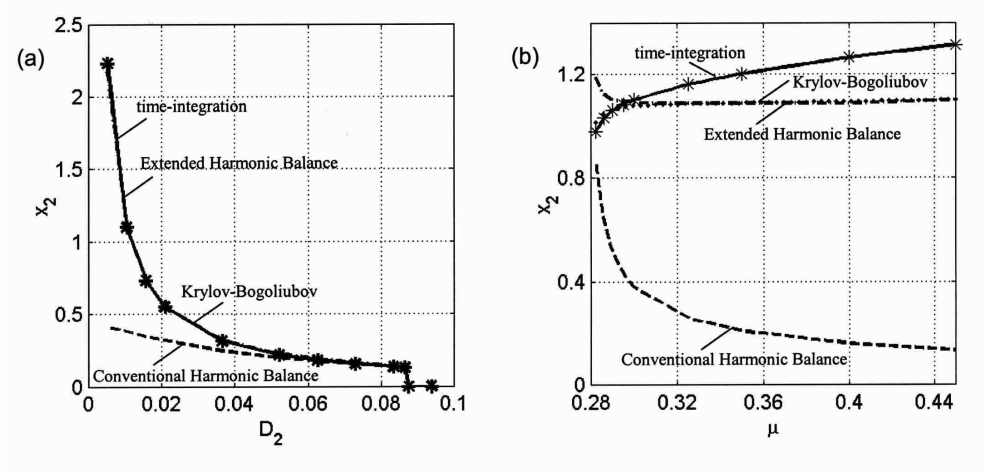

Figure 5. Benchmark of the approximate techniques (Conventional Harmonic Balance: dashed, Extended Harmonic Balance: dash-dotted, Krylov-Bogoliubov: dotted) vs. the result from direct time-integration (solid). (a) x_2-amplitude vs. damping coefficient D_2. (b) x_2-amplitude vs. friction-coefficient μ.

Let us first discuss the techniques' performance with respect to predicting satisfying values for the x_2-vibration when damping is varied, see figure 6 (a). Obviously both the Extended Harmonic Balance approach as well as Krylov-Bogoliubov perform extremely well, hardly any difference to the results from direct time integration can be determined by the eye. However, conventional Harmonic Balance yields - for small damping coefficients - values for the x_2-vibration that are substantially below the correct ones. Of course this benchmark has been chosen deliberately to detect, which of the techniques copes satisfactorily with the effect already described in the introduction, that the x_2-vibration somehow decouples from the x_1-vibration when stick-slip sets in. Following this reasoning it is clear that conventional Harmonic Balance will yield poor results, especially for low damping situations, since it does not allow for a change in the ratio of x_1- and x_2-amplitudes but sticks to the ratio given from eigenvalue analysis of the linearized system even in the regime of strong nonlinearity. The other two techniques do allow the nonlinearity to adjust the ratio of x_1 and x_2 and consequently yield excellent results in this benchmark.

The second benchmark performed focuses more on the capability of the techniques to take the non-linearities inherent in the system into account. For that purpose the friction coefficient μ has been varied, all other parameters staying constant. The results are given in figure 6 (b), where the x_2-amplitude is now represented vs. the friction coefficient μ. Obviously conventional Harmonic Balance performs rather poorly, mainly because of the shortcomings already described above. Both Extended Harmonic Balance as well as Krylov-Bogoliubov lead to comparable results, although for larger values of μ they consistently underestimate the x_2-amplitude. Close to the onset of instability Krylov-Bogoliubov seems to perform a bit better than the Extended Harmonic Balance.

6 Summary, Conclusions and Outlook

Three techniques to approximately determine the limit-cycle amplitudes of stick-slip vibrations in a mode-coupling unstable two-degree-of-freedom system have been evaluated and compared. It has turned out that the vibration characteristics, especially the mean ratios of vibration component amplitude, of the stationary limit-cycle state may differ substantially from what might be expected from a stability analysis of the steady sliding state and its corresponding most unstable eigenvector.

Consequently application of the conventional Harmonic Balance approach, adjusted only slightly to the two-degree-of-freedom problem at hand, does not yield satisfactory results, especially with respect to those vibration components that are not linked directly to the dynamics of stick-slip. We have seen that in our model problem conventional Harmonic Balance may result in grossly incorrect values for the x_2-component of the vibration, which could however e.g. be crucial for the radiation of noise in the original or underlying noise and vibration problem of brake squeal to be investigated. Since in detailed applications it seems difficult to judge in advance the error that conventional Harmonic Balance brings with it, it does not seem to be a good candidate for approximately solving stick-slip problems in the context of mode-coupling unstable systems.

An extended Harmonic Balance, taking into account more degrees of freedom for the underlying ansatz functions, does not show the problem of the conventional Harmonic Balance and yields results comparable to those of the technique of Krylov-Bogoliubov. Both approaches yield quite good results for the dynamics related to the sticking-dynamics (i.e. the x_1-component in the present example), nevertheless there do remain substantial errors with respect to components not directly tied to the sticking dynamics (i.e. the x_2-components in our example), since they both assume harmonic oscillation behavior and therefore can take into account the non-harmonic distortions so characteristic for stick-slip vibrations only to a limited extent. Nevertheless their results seem promising for use in engineering contexts, where other modeling and simulation uncertainties can definitely lead to the same order of modeling uncertainty as the approaches described. However, both approaches lead to non-linear sets of equations that have to be solved by iterative algorithms. Moreover the formal mathematical effort that has to be taken is rather large, especially in the case of Krylov-Bogoliubov.

It therefore seems appropriate to conclusively discuss the role that techniques like the ones described might play in the application on engineering problems in an everyday engineering work-process. It has been stated already in the introduction that although computer power is still increasing exponentially over time, many problems, especially large-scale friction affected systems like the ones that motivated the present work, do still not allow evaluation of limit-cycle behavior on a routine basis, although corresponding results would be urgently necessary, e.g. to reliably predict the noise radiation of rolling automotive tyres, automotive friction brakes or the wheel/rail system. A number of solutions to the problem can of course be imagined, and the use of approximative techniques like those described in the present work is one option only. Most prominent alternative approaches are: (1) Direct time integration in the framework of finite-element analysis: Depending on the complexity of the problem under consideration, this option will probably be restricted to not too complex friction situations, as experience shows. (2) Direct time integration after use of condensation techniques: this is a very promising approach, however the sometimes strange peculiarities of friction processes might make it difficult to find generic condensation strategies yielding generically satisfying results. (3) Use of Elastic Multibody Simulation: an increasingly popular approach, which however faces similar problems as the approach based on finite-elements and condensation. The present work might be regarded as a contribution to a fourth approach, which could be based on some rather standard preprocessing steps (like determination of a steady sliding state and afterwards an eigenvalue analysis to determine system stability information) supplemented by some sort of quick and computationally efficient post-processing based on approximative techniques, yielding results on limit-cycle amplitudes.

Of course the results shown do not yet describe the full process chain leading to finite-amplitude limit-cycle results in the context of friction self-excited systems. Rather, the present work has focused on a benchmark of the algorithms that might, and that might not play a role in such a process. In addition, further questions will have to be answered, before a final evaluation of such a process can be performed: (1) How can the multi-degree-of-freedom problem as it is found e.g. in large finite-element calculations be projected on a few-degree-of-freedom problem, that might allow approximate techniques to be used? Basically this is the question of reduction of degrees of freedom. (2) Even after an appropriate few-degree-of-freedom representation of the system under consideration has been set up, there are still several options for the application of approximation techniques: In the present work the techniques have been applied directly to a minimal two-degree-of-freedom model in physical coordinates. Of course an analogous approach could be taken for modal coordinates or other reduced systems.

It will be the task of further studies to determine, if an approach like sketched above may be able to compete with the rapidly progressing finite-element and multibody modeling and simulation techniques. For very large scale friction affected dynamic systems however there could be the possibility that an approach making use of the elegant, sometimes intricate, but always very efficient mathematics of approximate techniques might - adapted to and included in the powerful framework of commercial tools - outperform alternative conventional techniques to determine non-linear limit-cycle behavior.

References

Allgaier, R.; Gaul, L.; Keiper, W.; Willner, K.; Hoffmann, N.: A study on brake squeal using a beam-on-disc model. In: *IMAC XX, CD-ROM*, Kissimee (2002).

Gasparetto, A.: Eigenvalue analysis of mode-coupling chatter for machine-tool stabilization. *J. of Vibration and Control*, 7, (2001), 181 – 197.

Gaul, L.; Nitsche, R.: Role of friction in mechanical joints. *Applied Mechanics Reviews*, 54, (2001), 93 – 105.

Hoffmann, N.; Fischer, M.; Allgaier, R.; Gaul, L.: A minimal model for studying properties of the mode-coupling type instability in friction induced oscillations. *Mechanics Research Communications*, 29, (2002), 197 – 205.

Hoffmann, N.; Gaul, L.: Effects of damping on mode-coupling instability in friction induced oscillations: imperfect merging of modes and viscous instability. *Z. Angew. Math. Mech.*, 83, (2003), 524 – 534.

Ibrahim, R. A.: Friction-induced vibration, chatter, squeal and chaos, part ii: dynamics and modeling. *ASME Applied Mechanics Reviews*, 47, (1994), 227 – 253.

Magnus, K.; Popp, K.: *Schwingungen*. Teubner, Stuttgart (1997).

Nayfeh, A. H.; Mook, D. T.: *Nonlinear Oscillations*. John Wiley & Sons, New York (1995).

Popp, K.; Stelter, P.: Stick-slip and chaos. *Philosophical Transactions of the Royal Society London A*, 332, (1990), 89 – 105.

Schroth, R.: *Zum Entstehungsmechanismus des Bremsenquietschens*. VDI Verlag, Düsseldorf (2003).

Spurr, R. T.: A theory of brake squeal. *Proceedings of the Automotive Division, Institute of Mechanical Engineers (AD)*, 1, (1961), 33 – 40.

Wallaschek, J.; Hach, K.-H.; Stolz, U.; Mody, P.: A survey of the present state of friction modelling in the analytical and numerical investigation of brake noise generation. In: A. Guran; J. Wegner, eds., *Proceedings of the ASME Vibration Conference*, Birkhäuser, Las Vegas (1999).

Address: Institut A für Mechanik, Universität Stuttgart, Pfaffenwaldring 9, D-70550 Stuttgart.
email: `norbert.hoffmann2@de.bosch.com, l.gaul@mecha.uni-stuttgart.de`